Lecture 19, the structure of neutron stars

summary of neutron star properties

- The densest objects this side of an event horizon, with a mean density $\approx 10^{15}$ g cm^{-3}. Four teaspons contain as much mass as the Moon.
- The largest surface gravity, about 10^{14} cm s^{-2}, or 100 billion times Earth's gravity.
- The fastest spinning macroscopic objects. A pulsar, PSR J1748-2446ad in the globular cluster Terzan 5, has a spin rate of 714 Hz [1], so that its surface velocity at the equator is about $c/4$.
- The larges magnetic field strength, of order 10^{15} G.
- The highest temperature superconductor, with a critical temperature of a few billion K, has been deduced for the core superfluid neuitrons in the remnant of the Cassiopeia A supernova [2, 3].
- The highest temperatures, outside the Big Bang, exist at birth or in merging neutron stars, about 700 billion K.
- The pulsar PSR B1508+55 has a spatial velocity in excess of 1100 km s^{-1} [4].
- Neutron stars at birth or in matter from merging neutron stars are the only places in the universe, apart from the Big Bang, where neutrinos become trapped and must diffuse through high density matter to eventually escape.

70 MeV

actually, we measure T > 150 MeV in relativistic nuclear collisions
on earth (at RHIC and CERN)

numbers to remember:
there are approximately 100 million neutron stars and
approximately 360 billion stars in the milky way
approximately 2000 have been identified

computer simulation of a spinning neutron star, with electric and magnetic field lines
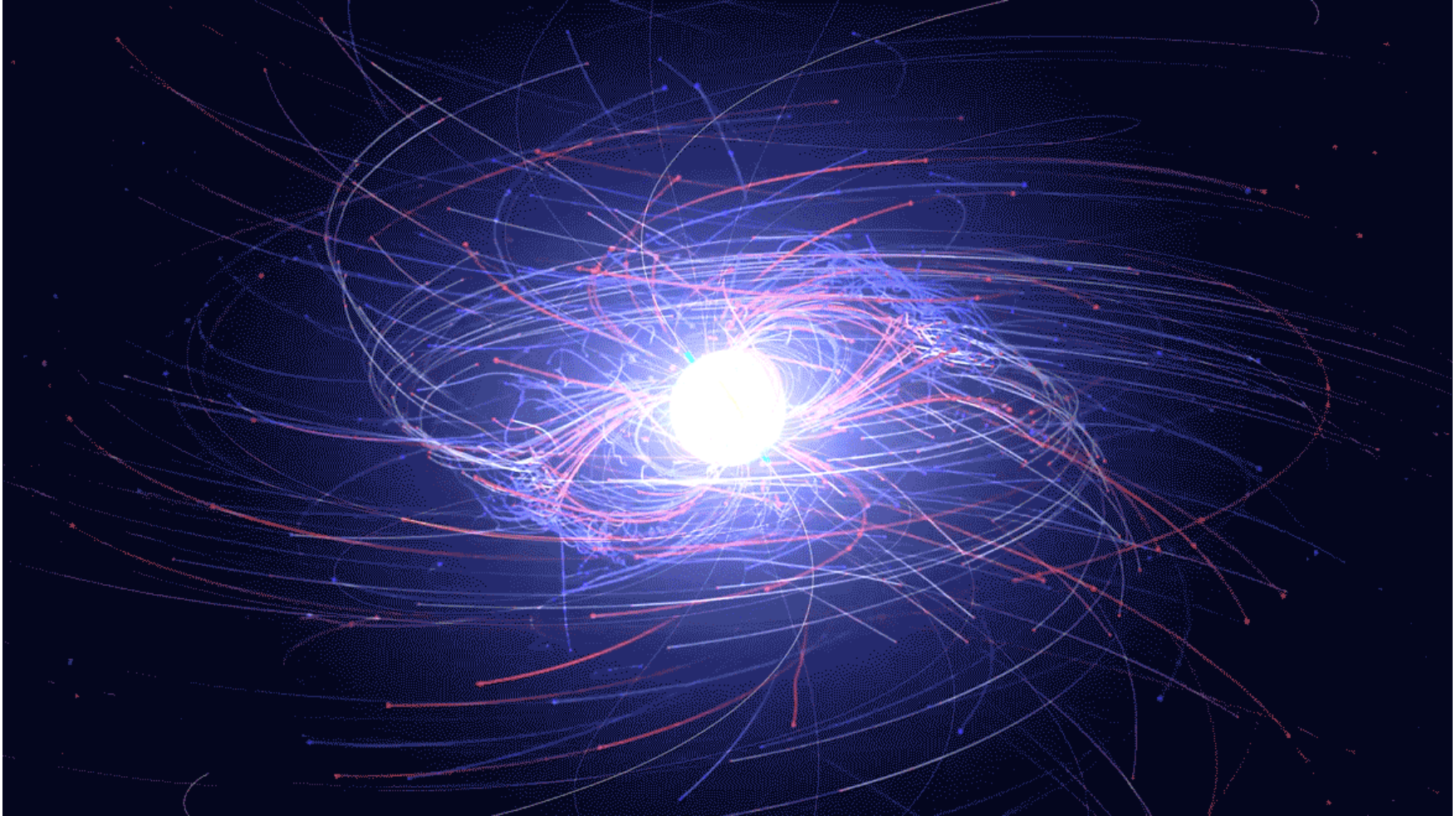
Credit: NASA's Goddard Space Flight Center

Historical comments on 'neutron stars'

1920 Rutherford predicts existence of the neutron. *in the 1920 'Bakerian lecture of the Royal Society*

1931 Landau anticipates single-nucleus stars (not precisely neutron stars). *L.D. Landau, Phys. Z. Sowietunion 1 (1932) 285*

1932 Chadwick discovers the neutron.

1934 W. Baade and F. Zwicky [5] suggest that neutron stars are the end product of supernovae.

1939 Oppenheimer and Volkoff [6] find that general relativity predicts a maximum mass for neutron stars.

1964 Hoyle, Narlikar and Wheeler [7] predict that neutron stars rotate rapidly.

1965 Hewish and Okoye [8] discover an intense radio source in the Crab nebulae, later shown to be a neutron star.

1966 Colgate and White [9] perform simulations of core-collapse supernovae resulting in formation of neutron stars.

1967 C. Schisler discovers a dozen pulsing radio sources, including the Crab, using classified military radar. He revealed his discoveries in 2007. Later in 1967 Hewish, Bell, Pilkington, Scott and Collins [10] discover PSR 1919+21 (Hewish receives 1974 Nobel Prize). *actually, Jocelyn Bell, grad. student of A. Hewish, makes the discovery mostly on her own*

1968 Crab pulsar discovered [11] and pulse period found to be increasing, characteristic of spinning stars but not binaries or vibrating stars. This also clinched the connection with supernovae. The term 'pulsar' first appears in print in the *Daily Telgraph*.

1969 "Glitches" observed [12], providing evidence for superfluidity in the neutron star crust [13].

1971 Accretion powered X-ray pulsars discovered by the Uhuru satellite [14].

1974 The first binary pulsar, PSR 1913+16, discovered by Hulse and Taylor [15] (Nobel Prize 1993). It's orbital decay is the first observation [16] proving existence of gravitational radiation. Lattimer and Schramm [17] suggest decompressing neutron star matter from merging compact binaries leads to synthesis of r-process elements.

1982 The first millisecond pulsar, PSR B1937+21, discovered by Backer et al. [18]

1996 Discovery of the closest neutron star RX J1856-3754 by Walter et al. [19].

1998 Kouveliotou discovers the first magnetar [20].

references for historical comments

1. J. W. T. Hessels et al. *Science* **311**, 1901 (2006).
2. D. Page, M. Prakash, J. M. Lattimer and A. W. Steiner, *Phys. Rev. Lett.* **106**, 081101 (2011).
3. P. S. Shternin, D. G. Yakovlev, C. O. Heinke, W. C. G. Ho and D. J. Patnaude, *MNRAS* **412**, 108 (2011).
4. S. Chatterjee et al., *ApJ Lett.* **630**, L61 (2005).
5. W. Baade and F. Zwicky, *PNSA* **20**, 259 (1934).
6. J. R. Oppenheimer and G. M. Volkoff, *Phys. Rev.* **55**, 374 (1939).
7. F. Hoyle, J. V. Narlikar and J. A. Wheeler, *Nature* **203**, 914 (1964).
8. A. Hewish and S. E. Okoye, *Nature* **207**, 59 (1965).
9. S. A. Colgate and R. H. White, *ApJ* **143**, 626 (1966).
10. A. Hewish, S. J. Bell, J. D. H. Pilkington, P. F. Scott and R. A. Collins, *Nature* **217**, 709 (1968).
11. J. M. Comella, H. D. Craft, R. V. E. Lovelace and J. M. Sutton, *Nature* **221**, 453 (1969).
12. V. Radhakrishnan and R. N. Manchester, *Nature* **222**, 228 (1969); P.E. Reichley and G. S. Downs, *Nature* **222**, 229 (19
13. G. Baym, C. Pethick and D. Pines, *Nature* **224**, 673 (1969).
14. R. Giacconi et al., *ApJ Lett.* **167**, L67 (1971).
15. R. A. Hulse and J. H. Taylor, *ApJ* **195**, 51 (1975).
16. J. H. Taylor, L. A. Fowler and P. M. McCulloch, *Nature* **277**, 437 (1979).
17. J. M. Lattimer and D. N. Schramm, *ApJ Lett.* **192**, L145 (1974).
18. D. C. Backer, S. R. Kulkarni, C. Heiles, M. M. Davis and W. M. Goss, *Nature* **300**, 615 (1982).
19. F. M. Walter, J. S. Wolk and R. Neuhäuser, *Nature* **379**, 233 (1996).
20. C. Kouveliotou et al., *Nature* **393**, 235 (1998).

mass and radius of a neutron star

determined via solution of Tolman-Oppenheimer-Volkoff equations, see Lect. 18, by specifying the equation of state $P = P(T, \rho, Y_e)$

$$\frac{dP}{dr} = -\frac{G(m(r) + 4\pi r^3 P/c^2)(\rho + P/c^2)}{r(r - 2Gm(r)/c^2)}$$

$$\frac{dm(r)}{dr} = 4\pi \rho r^2$$

this set of differential equations can, for practical cases, only be solved numerically

mass and radius of a neutron star

determined via solution of Tolman-Oppenheimer-Volkoff equations, see Lect. 18, by specifying the equation of state $P = P(T,\rho,Y_e)$

$$\frac{dP}{dr} = -\frac{G(m(r) + 4\pi r^3 P/c^2)(\rho + P/c^2)}{r(r - 2Gm(r)/c^2)}$$

$$\frac{dm(r)}{dr} = 4\pi \rho r^2$$

this set of differential equations can, for practical cases, only be solved numerically

modern version of mass-radius relationship of neutron stars
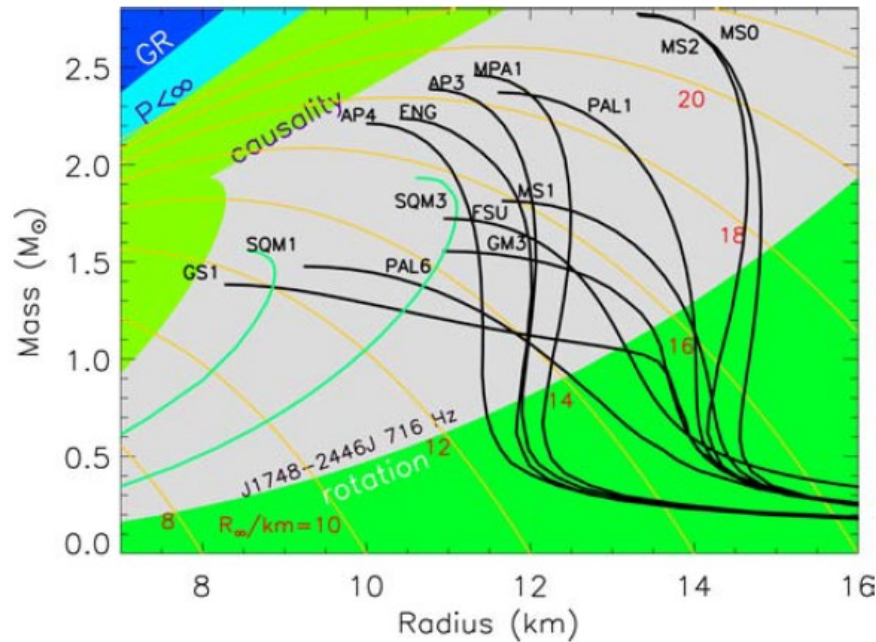
fig. from J. Lattimer,

Mass–radius curves for a variety of popular EOSs (see Ref. 8 for descriptions). The green shaded region in the upper left is causally excluded; the green shaded region in the lower-right is excluded by the most rapidly spinning pulsar. Black curves are hadronic EOSs; green curves are for strange quark matter configurations. Lines of fixed $R_\infty = R/\sqrt{1-2\beta}$ are indicated as orange curves.

these curves imply that neutron star radii will be somewhere between 8 and 14 km, but how can one make precision measurements of mass and radius?

mass measurements via Shapiro delay
in binary systems

P. Demorest et al.,   Nature 467 (2010) 1081-1083

'The Shapiro delay is an increase in light travel time through the curved space-time near a massive body. In binary pulsar systems that have highly inclined (nearly edge-on) orbits, excess delay in the pulse arrival times can be observed when the pulsar is situated nearly behind the companion dur-ing orbital conjunction. As described by general relativity, the two physical parameters that characterize the Shapiro delay are the companion mass and inclination angle. In combination with the observed Keplerian mass function, the Shapiro delay oﬀers one of the most precise methods to directly infer the mass of the NS.'

animated picture for Shapiro delay courtesy Wikimedia Commons, Author:Yukterez (Simon Tyran, Vienna)

t = 0.000 GM/c³

yukterez
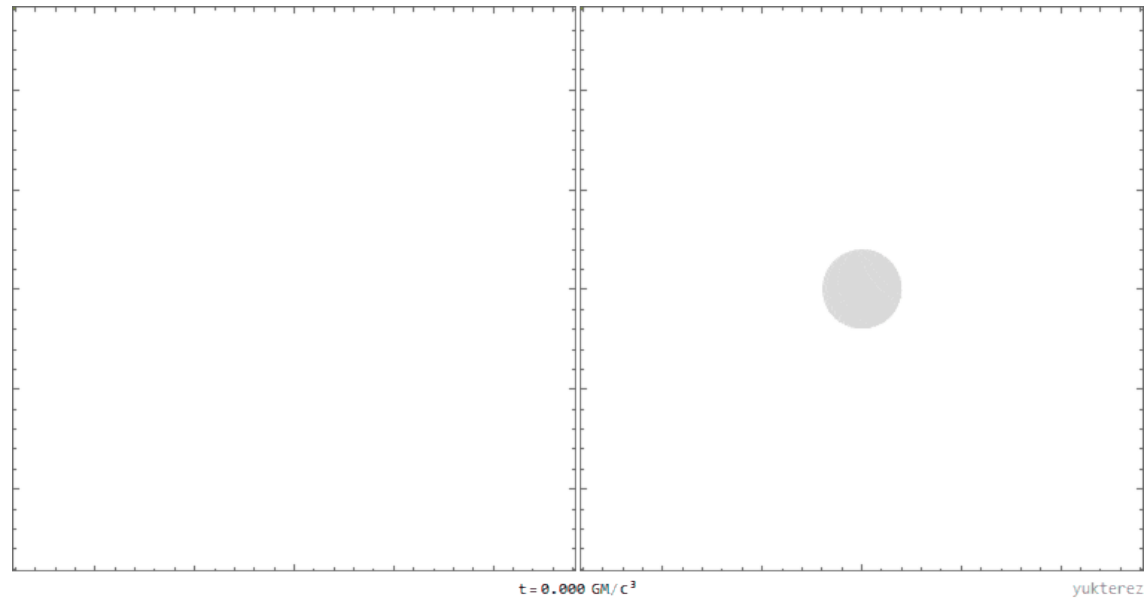
Shapiro delay measured for the Venus-Sun-Earth system

$$\Delta t = \frac{2GM}{c_0^3} \ln \left[\frac{x_E + r_E}{x_P + r_P} \right] = \frac{2GM}{c_0^3} \ln \left[\frac{(r_E + \vec{n} \cdot \vec{x}_E)(r_P - \vec{n} \cdot \vec{x}_P)}{\eta^2} \right]$$
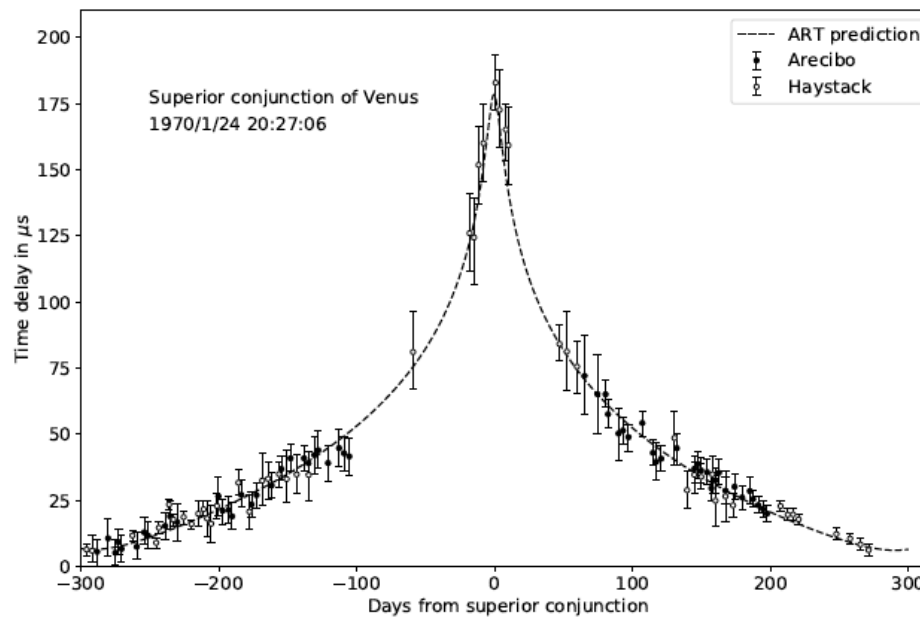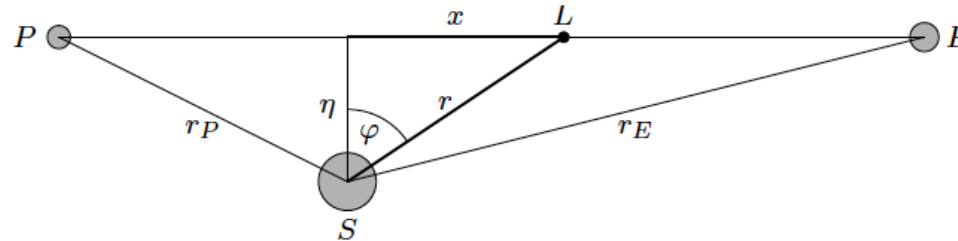
Comparison between the prediction of (27) and Shapiro's radar echo data for Venus from 1970/1971

figures taken from: M. Poessel, arXiv:2001.00229. This paper also contains a pedagogical derivation of the above delay formula.

Shapiro delay measurements for pulsar PSR J1614−2230
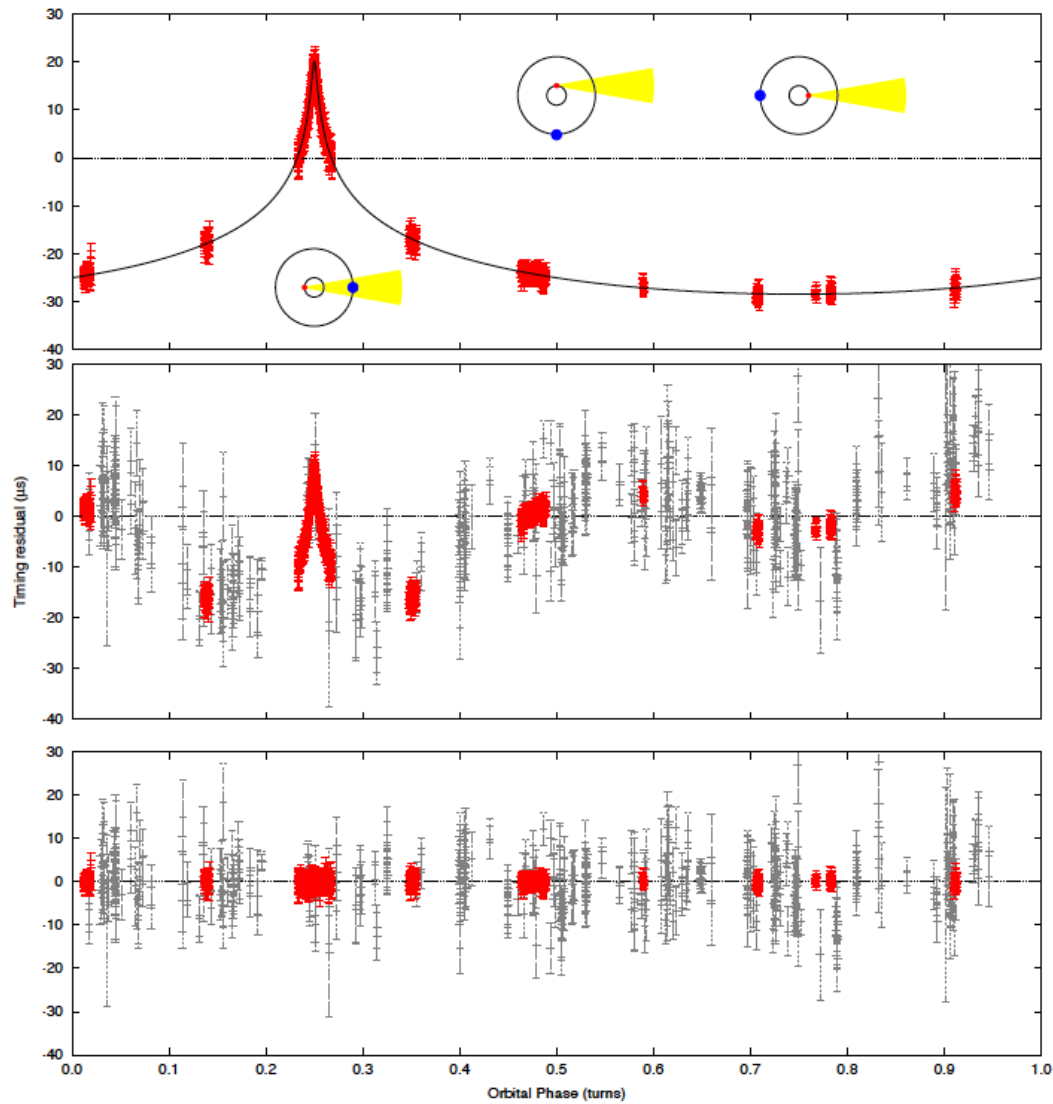
Nature 467 (2010) 1081-1083

geometry for a binary system containing a pulsar

In the Deforest case, the inclination angle i = 89.17 ± 0.02 deg. so luckily the Shapiro delay is maximal
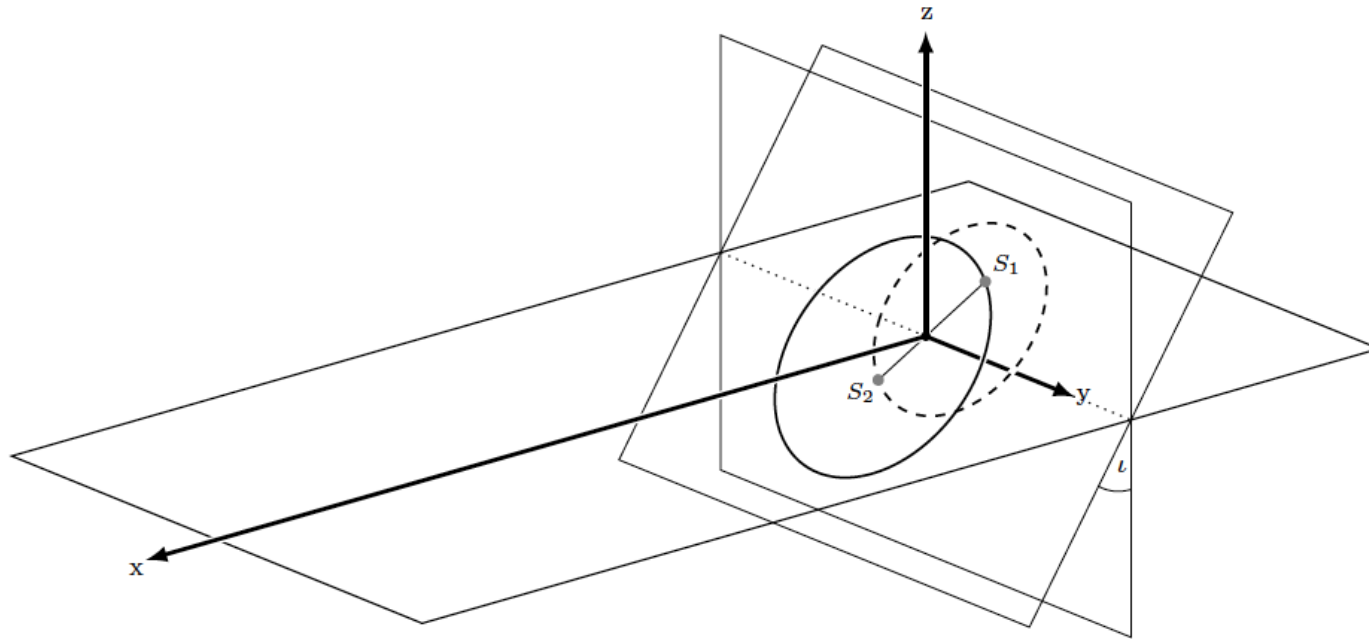
Binary containing a pulsar, as seen from Earth. The orbital plane of the stars is inclined relative to the yz plane by the inclination angle ι

from the 8.7 day orbital period of the binary (obtained via Doppler shift measurements of the pulsar frequency) and the mass of the companion star (a while dwarf) obtained via Shapiro delay, the mass of the neutron star is obtained

results:

Demorest et al.

$m_{ns} = 1.97 \pm 0.04\ m_\odot$

$m_{companion} = 0.50 \pm 0.006\ m_\odot$

orbital period of binary = 8.7 days

pulsar spin period = 3.15 ms

discovery of a 2 solar mass neutron star

Neutron star binaries and evidence for gravitational radiation will be dealt with in Lect. 20

two new mass measurements:

1. J. Antoniadis et al., Science 340 (2013) 6131

'We report the measurement of a 2.01±0.04 solar mass pulsar in a 2.46-hr orbit with a 0.172±0.003 solar mass white dwarf. The high pulsar mass and the compact orbit make this system a sensitive laboratory of a previously untested strong-field gravity regime. Thus far, the observed orbital decay agrees with GR, supporting its validity even for the extreme conditions present in the system. The resulting constraints on deviations support the use of GR-based templates for ground-based gravitational wave detectors. Additionally, the system strengthens recent constraints on the properties of dense matter and provides insight to binary stellar astrophysics and pulsar recycling.'

Neutron star binaries and evidence for gravitational radiation will be dealt with in Lect. 20

two new mass measurements:

1. J. Antoniadis et al.,   Science 340 (2013) 6131

'We report the measurement of a 2.01±0.04 solar mass pulsar in a 2.46-hr orbit with a 0.172±0.003 solar mass white dwarf. The high pulsar mass and the compact orbit make this system a sensitive laboratory of a previously untested strong-field gravity regime. Thus far, the observed orbital decay agrees with GR, supporting its validity even for the extreme conditions present in the system. The resulting constraints on deviations support the use of GR-based templates for ground-based gravitational wave detectors. Additionally, the system strengthens recent constraints on the properties of dense matter and provides insight to binary stellar astrophysics and pulsar recycling.'

2. H.T. Cromartie et al.,   Nature Astron. 4 (2019) 1, 72-76
arXiv :1904.06759

'By combining data from the North American Nanohertz Observatory for Gravitational Waves (NANOGrav) 12.5-year data set with recent orbital-phase-specific observations using the Green Bank Telescope,
we have measured the mass of the MSP J0740+6620 to be 2:14±0:10 solar masses (68.3% credibility interval; 95.4% credibility interval is 2:14±0:20 solar masses).'

Experimental approach to measure neutron star properties with NICER

key new idea: strong gravitational effects on the surface of neutron stars lead to distortion of X-ray images that provide new information on mass and radius of neutron stars

from: Anna Watts, arXiv:1904.07012
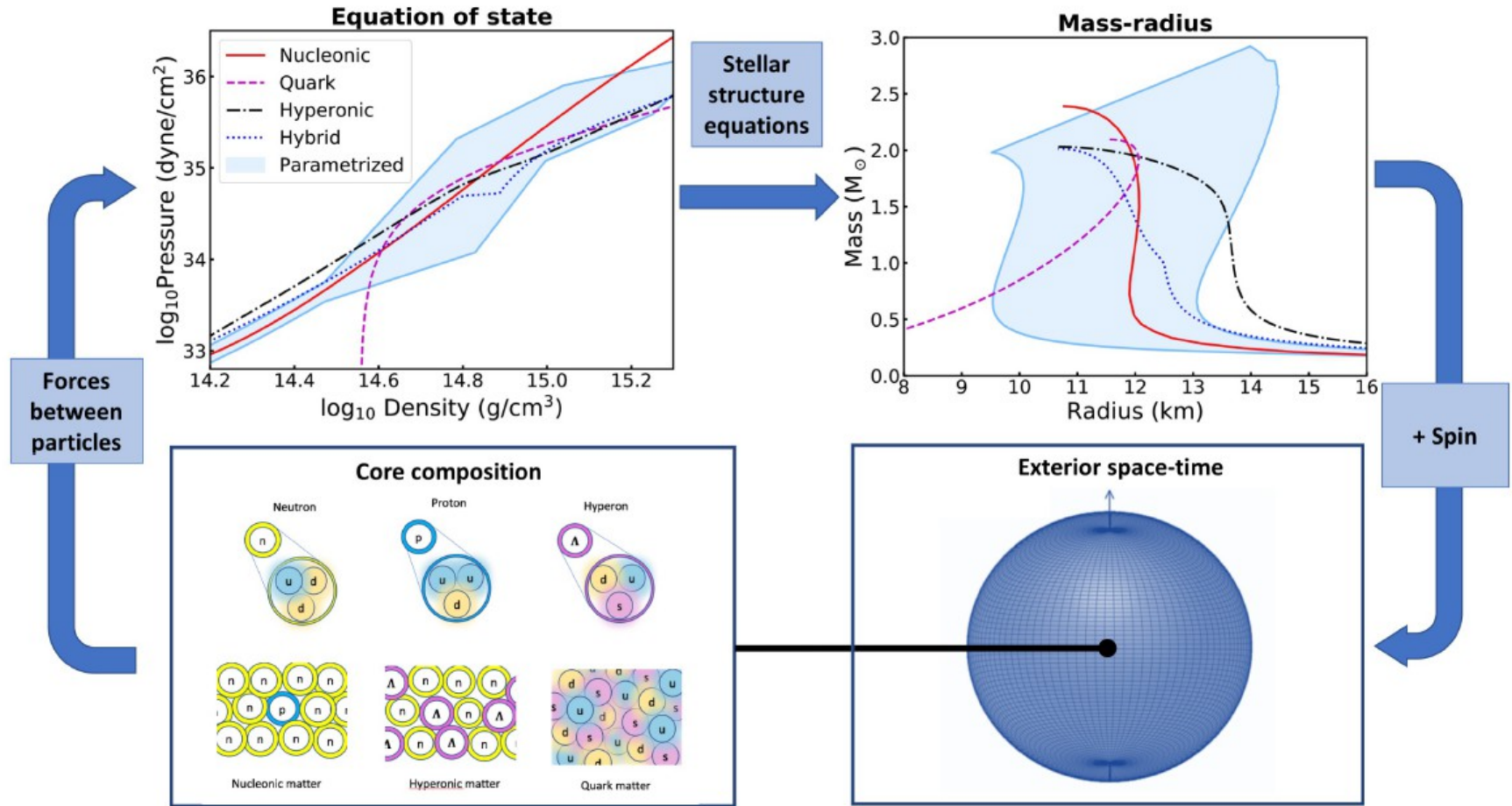
The relationship between the composition and inter-particle forces in the neutron star core, the EOS, the mass-radius relation, and the exterior space-time of the star. The space-time of the rotating neutron star imprints its signature on radiation emitted from the stellar surface: we can use this to infer the EOS.

note: surface temperature of young neutron star: 600000 K or 60 eV
hot spots can have many keV temperatures, X-ray emitters

NICER Mission Overview

- **Science:** An International Space Station (ISS) payload dedicated to the study of neutron stars. A fundamental investigation of extremes in gravity, material density, and electromagnetic fields

- **Launch:** June 3rd, 2017 at 17:07 EDT, on a SpaceX Falcon 9 rocket

- **Primary Mission Duration:** 18 months, with an additional 6 months long *Guest Observer program*

- **Platform:** ISS ExPRESS Logistics Carrier (ELC), with *active pointing* over 2π steradians

- **Instrument:** X-ray (0.2-12 keV) "concentrator" optics and silicon-drift detectors. GPS position and *absolute time reference* to better than 300 ns.

copy from NICER home page
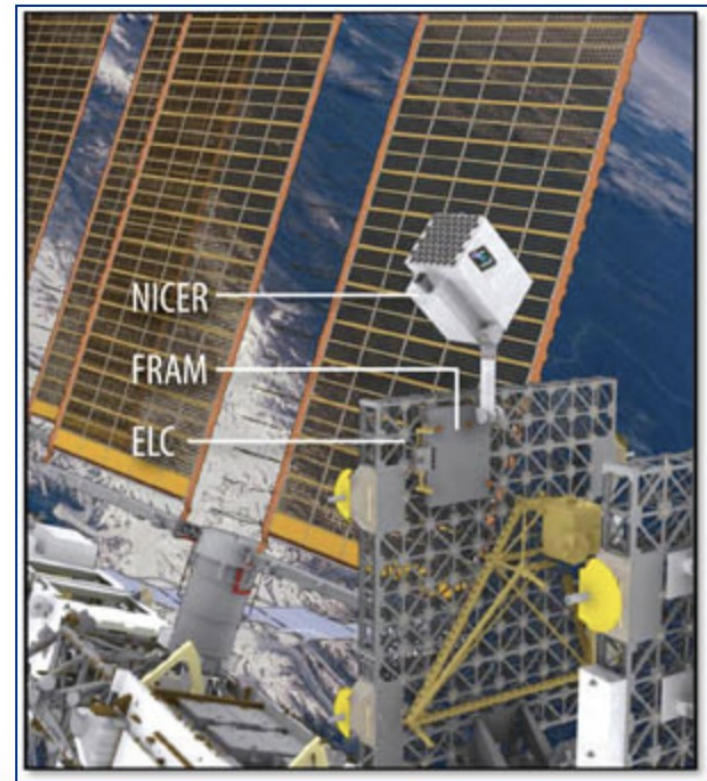
Warped image of a neutron star due to light deflection in the strong gravitational field
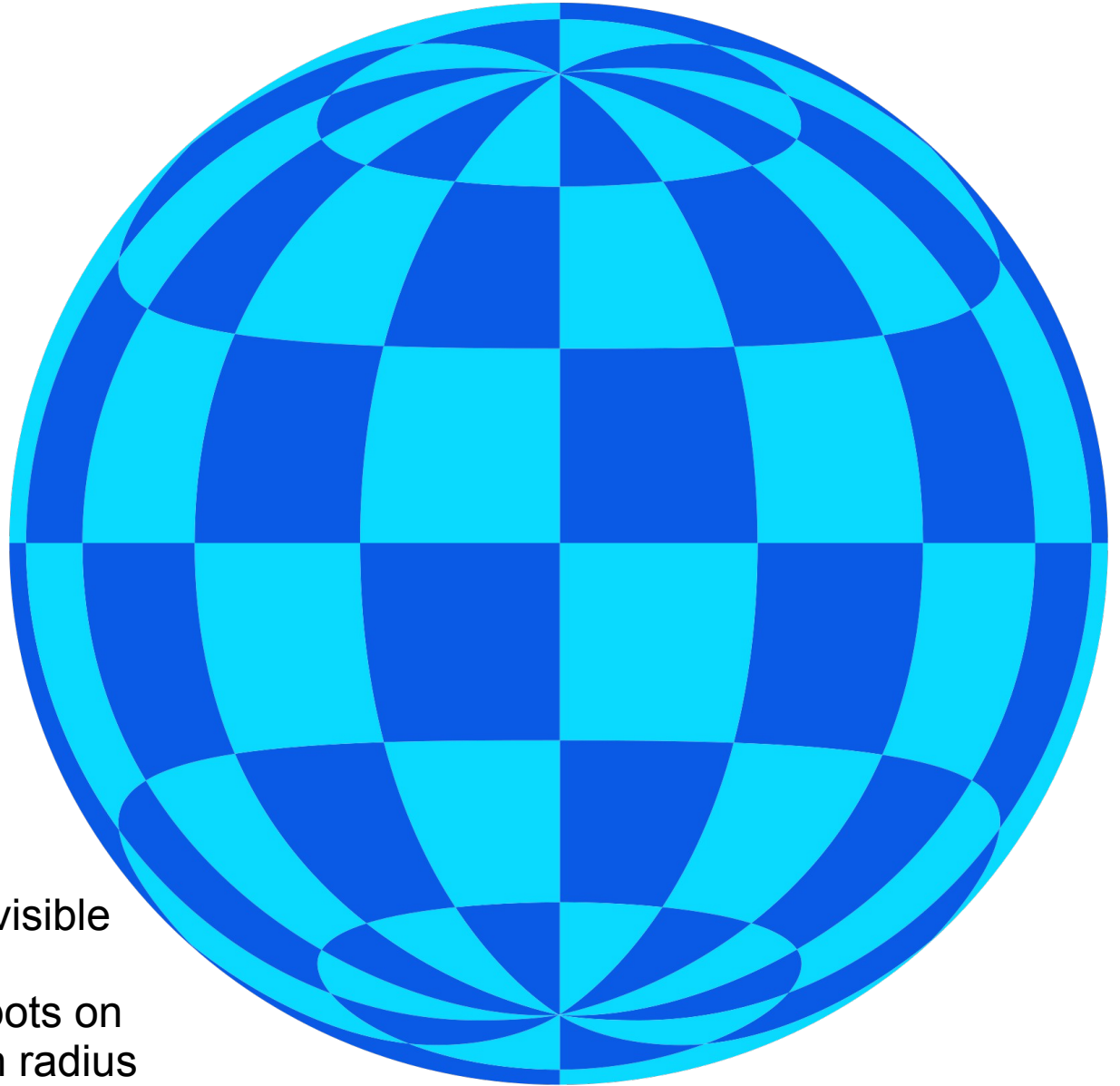
more than 1/2 of the surface is visible

imaging features such as hot spots on the surface gives information on radius and mass of the neutron star

The relativistic "looks" of a neutron star[*]

H.-P. Nollert, H. Ruder, H. Herold, and U. Kraus

Lehrstuhl für Theoretische Astrophysik der Universität Tübingen, Auf der Morgenstelle 12C, D-7400 Tübingen, Federal Republic of Germany
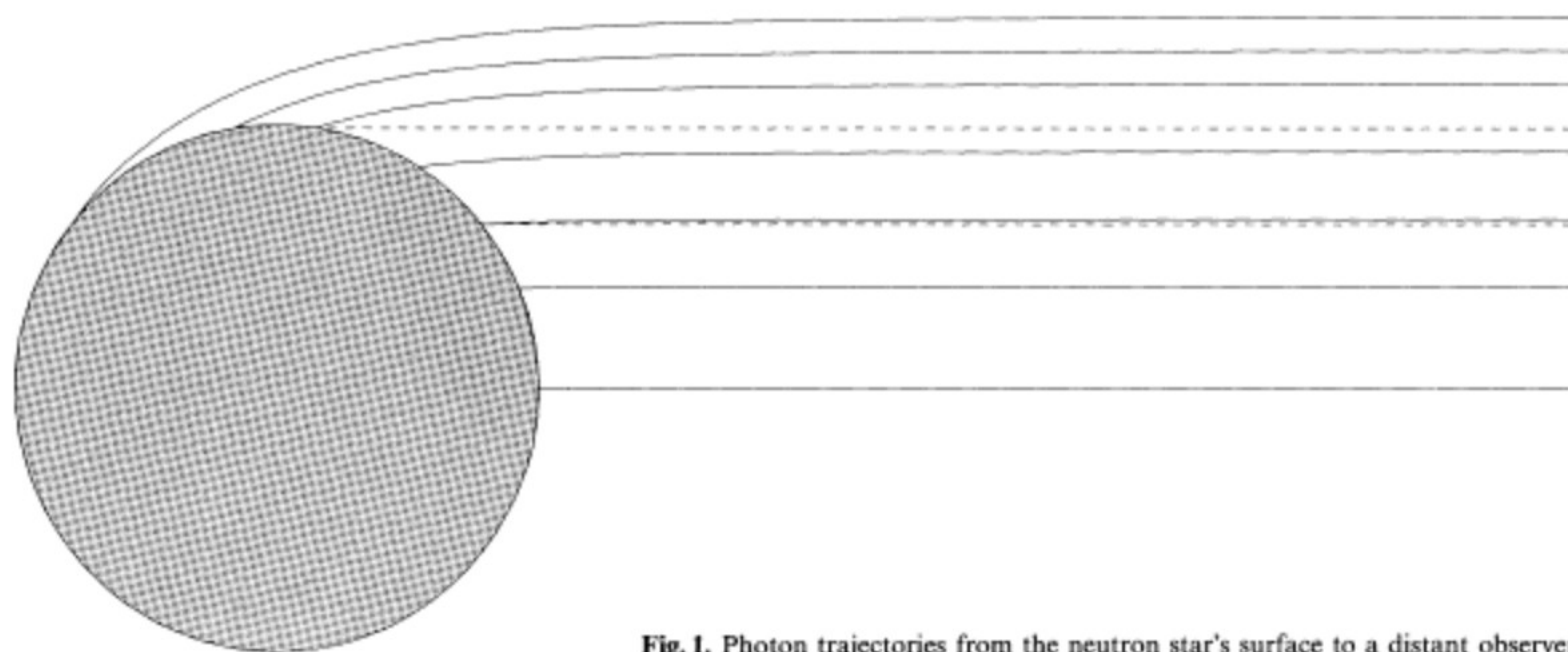
Fig. 1. Photon trajectories from the neutron star's surface to a distant observer

curvature of space depends on mass and radius of the object
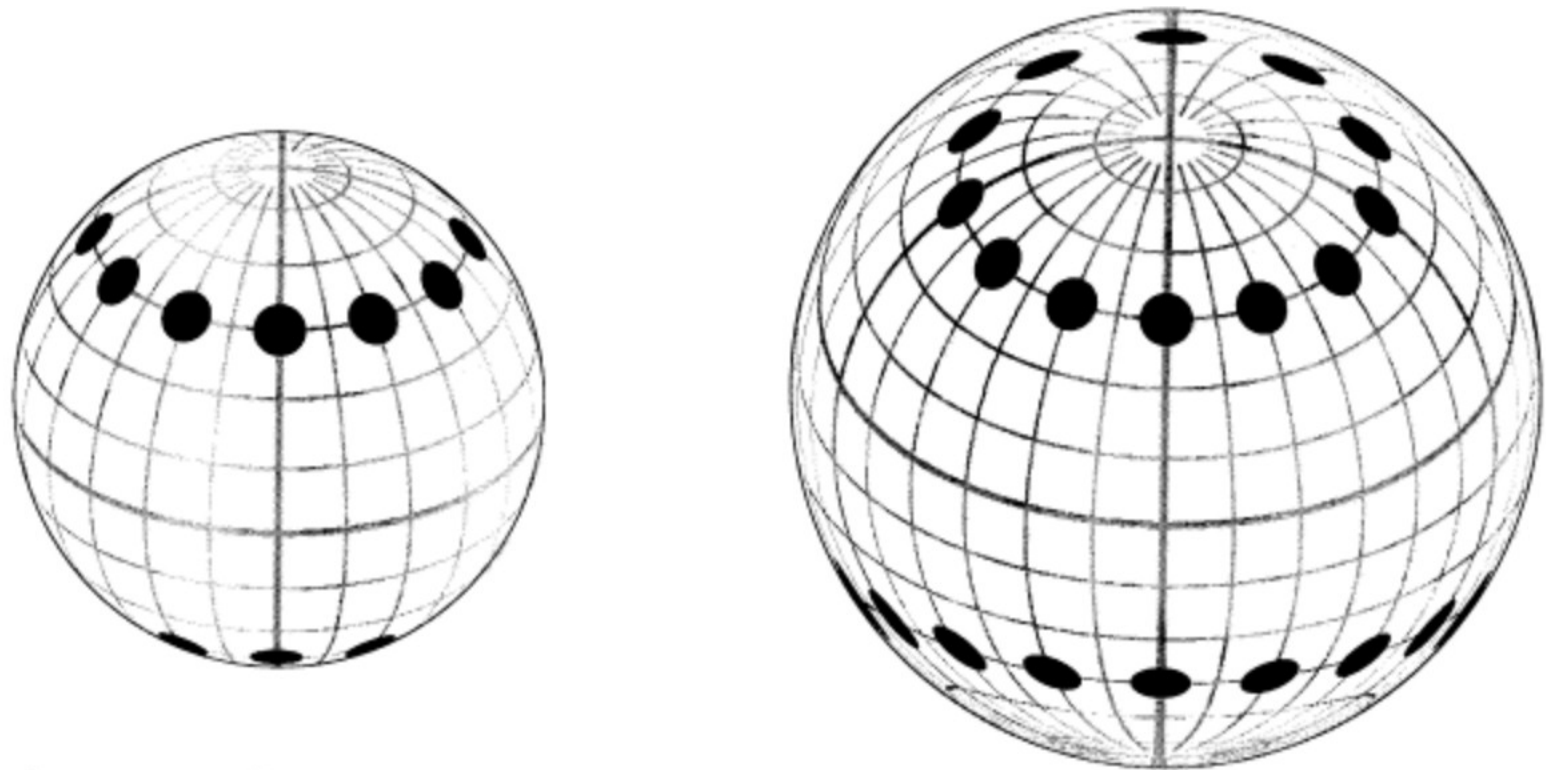
Fig. 3. Rotating neutron star with antipodal hot spots, $r_*/r_S = \infty$ (Minkowski case) and $r_*/r_S = 2$ for $\vartheta_p = 60°, \varphi_p = 90°, \vartheta_{hs} = 45°$

hot spots are created through relativistic gravitational lensing
see also next slide

hot spots on the surface of a rotating neutron star
Galin Gyulchev
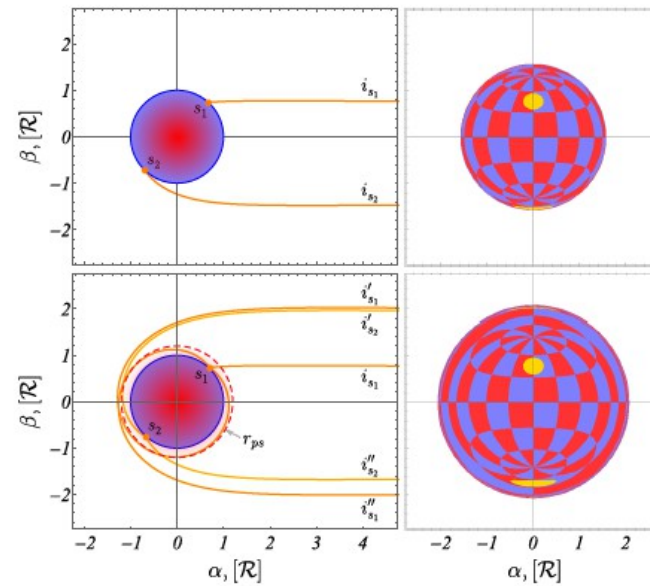
Photon's trajectories visualising the image creation of a hot spot on a neutron star with compactness $\mathcal{R}/2M = 1.7$ (*first row*) and formation of relativistic images of a hot spot on a neutron star possessing a photon sphere with compactness $\mathcal{R}/2M = 1.25$ (*second row*). The observer inclination angle is $\theta_{obs} = 90°$.

mass and radius of a neutron star from NICER measurements

from Anna Watts: Constraining the neutron star equation of state using Pulse Profile Modeling, arXiv:1904.07012

Dense matter with eXTP

pulse profile modeling
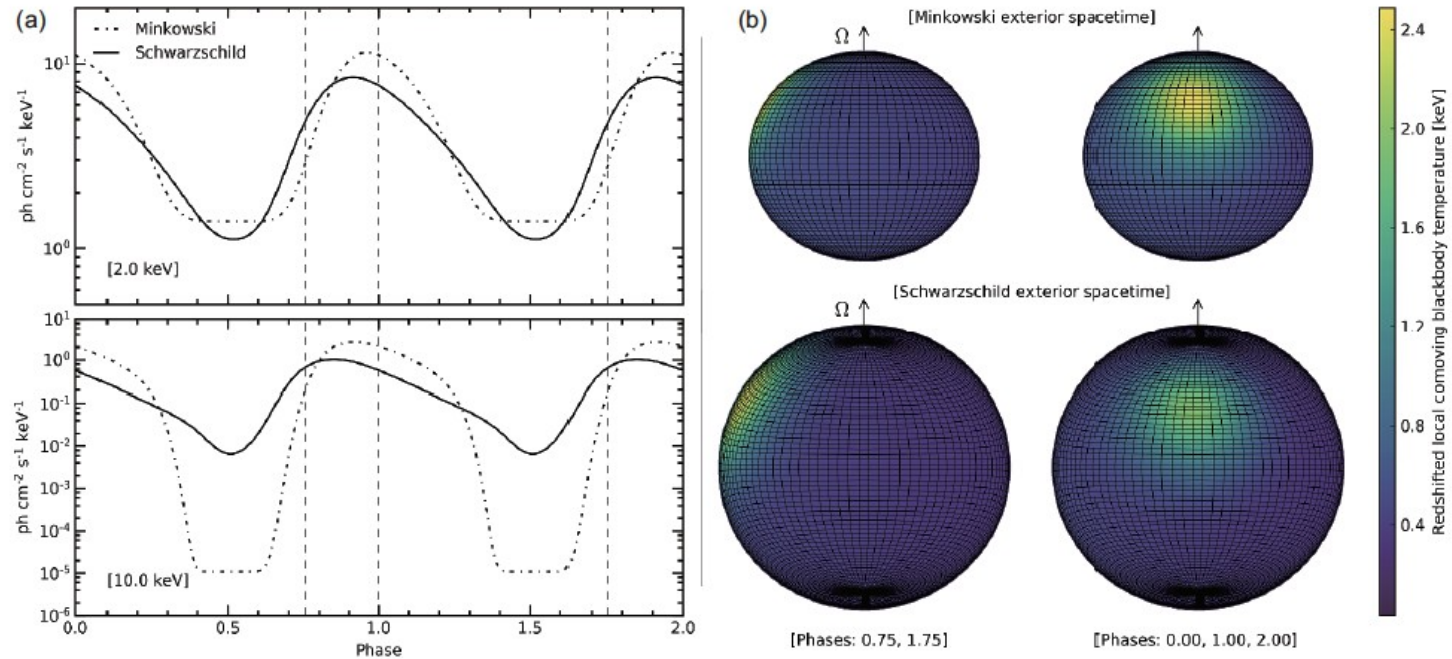
Stellar rotation modulates emission from a hot region (hotspot), generating an X-ray pulsation. Relativistic effects encode information about M and R in the normalisation and harmonic content of the pulse profile. These effects are key observables exploited by the pulse profile modelling technique, and include Doppler boosting and gravitational redshifting, time-delays, and light bending (which renders the far side of the star partially visible). The Figure illustrates these effects for a rapidly spinning, oblate star. We compare pulse profiles generated by a photosphere embedded in a Minkowski exterior spacetime to those generated by a photosphere embedded in a Schwarzschild exterior spacetime (see text). For the purpose of illustration, we use: a gravitational mass of $1.8\,M_\odot$; an equatorial coordinate radius of 14 km; a coordinate spin frequency of 600 Hz; and a distance of 1 kpc. The observer is in the equatorial plane. The local photospheric radiation field is completely specified by the local comoving blackbody temperature. The temperature field is non-evolving in the corotating reference frame, and is constituted by a hotspot of angular radius of 60°, centred at a colatitude of 60°. Its temperature falls smoothly from 2.5 keV at the centre to 0.5 keV at the boundary, where the latter is the temperature everywhere outside the spot boundary. (a) Monochromatic profiles at two energies (2-10 keV). (b) The resolved stellar photosphere at two rotational phases. The colour corresponds to the redshifted temperature on a distant image-plane.

measurements of X-ray hot spots with NICER
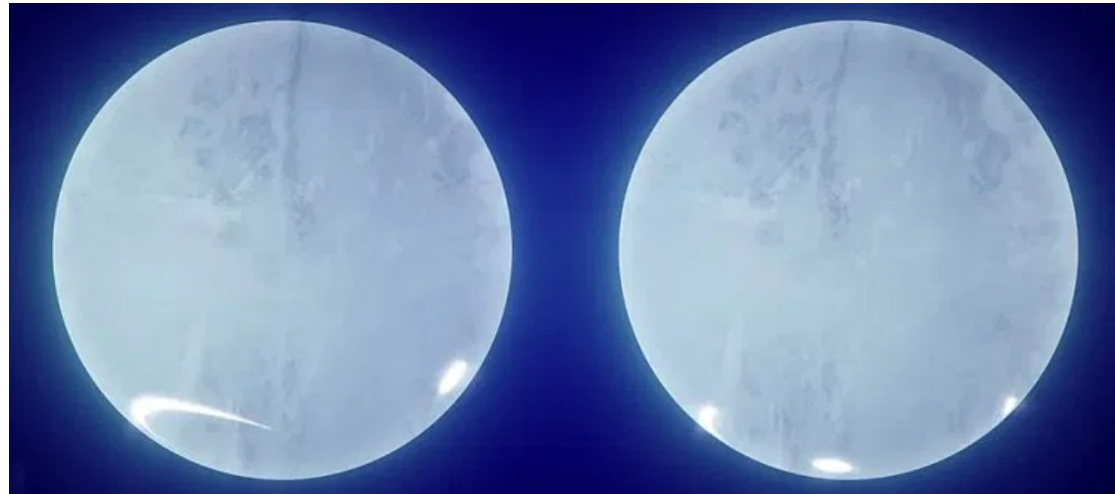
pulsar J0030
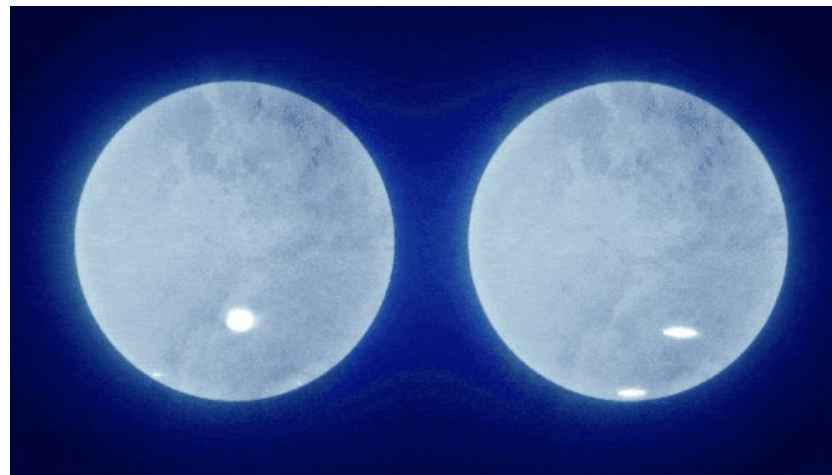
results of 2 different analyses of 1st NICER data: Amsterdam team (left), Maryland team (right)

results:

Amsterdam analysis: mass of neutron star = 1.3 $m_\odot$
radius of neutron star = 12.7 km

Maryland analysis: mass of neutron star = 1.4 $m_\odot$
radius of neutron star = 13.1 km

A NICER View of PSR J0030+0451: Millisecond Pulsar Parameter Estimation

Riley, T.E. et al., 2019, ApJL 887 L21.

A Nicer View of PSR J0030+0451: Implications for the Dense Matter Equation of State

Raaijmakers, G. et al., 2019, ApJL 887 L22.

schematic structure of the interior of neutron stars

outer crust 0.3-0.5 km
ions, electrons

inner crust 1-2 km
electrons, neutrons, nuclei

outer core ~ 9 km
neutron-proton Fermi liquid
few % electron Fermi gas

inner core 0-3 km
quark gluon plasma?

$0.3\text{-}0.5\ \rho_0$

$0.5\text{-}2.0\ \rho_0$

$>2.0\ \rho_0$
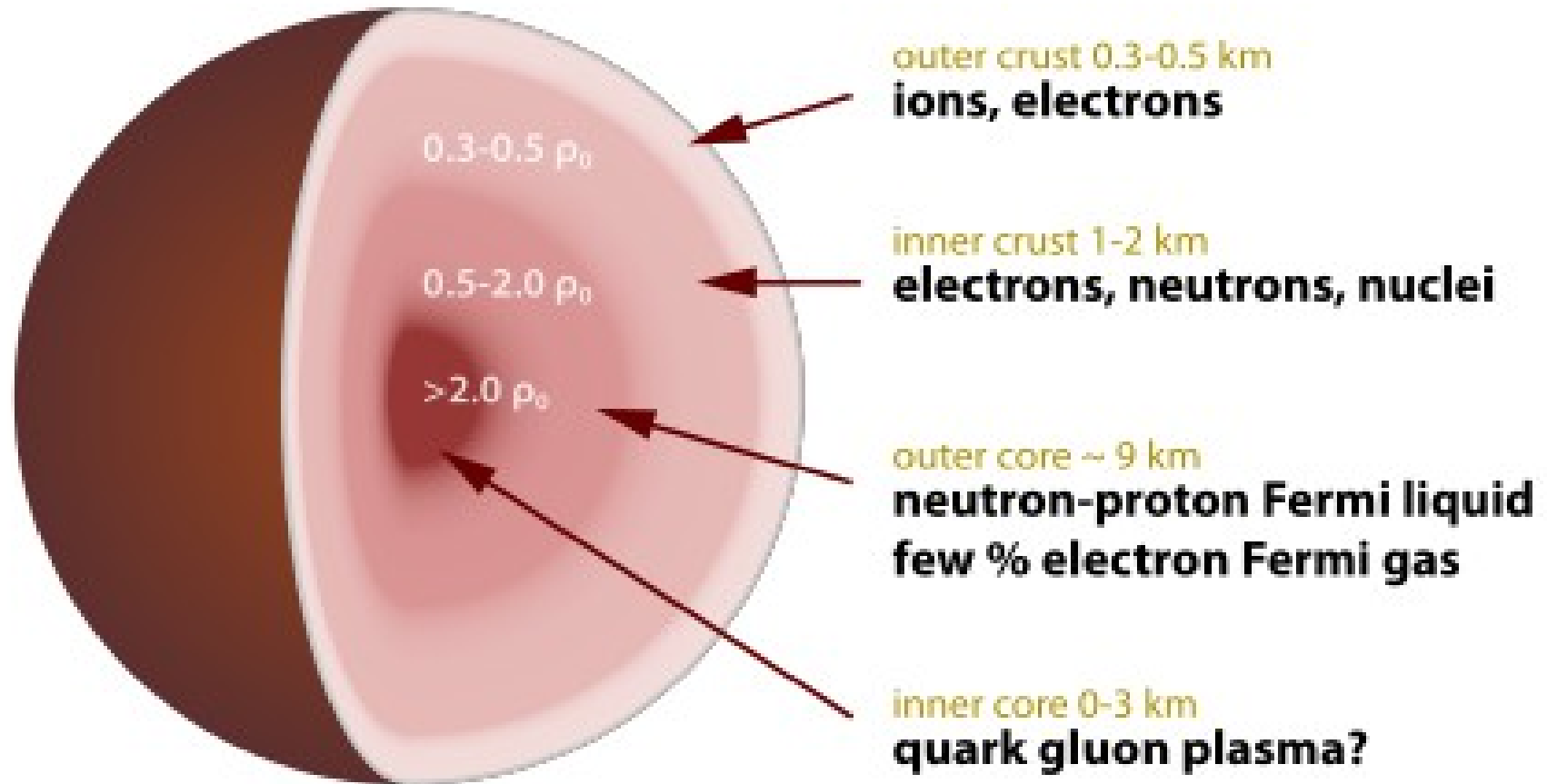
figure from wikipedia, CC BY-SA 3.0

structure in the outer crust: nuclear pasta shapes

figure taken from: C. Horowitz, M. Perez-Garcia, D. Berry and J. Piekarewicz,
`Dynamical response of the nuclear 'pasta' in neutron star crusts,'
Phys. Rev. C 72 (2005), 035801
arXiv:nucl-th/0508044 [nucl-th].
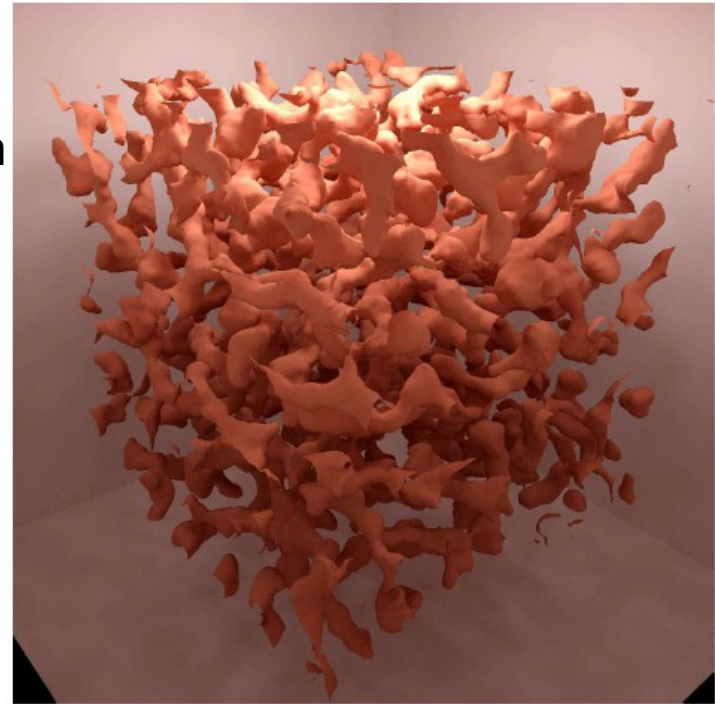
The 0.03 fm^{-3} proton density isosurface for one configuration of 100,000 nucleons at a baryon density of 0.05 fm^{-3}. The simulation volume is a cube of 126 fm on a side.